PLANT SCIENCE TODAY
Vol x(x): xx–xx
https://doi.org/10.14719/pst.8614

eISSN 2348-1900

RESEARCH ARTICLE

Molecular docking and dynamic simulation studies against the ERα of breast cancer using biomolecules from *Asparagus aethiopicus* L.

Aman Agrawal[1], Deepti Teotia[1], Vivek Kumar[1], Pooja Jain[1], Bhanu Agrawal[2], Ashish Kumar[1], Yeshvandra Verma[3] & Vijai Malik[1*]

[1]Department of Botany, Chaudhary Charan Singh University, Meerut 250 004, Uttar Pradesh, India
[2]BSA (PG) College, Dr. Bhim Rao Ambedkar University, Agra 282 004, Uttar Pradesh, India
[3]Department of Toxicology, Chaudhary Charan Singh University, Meerut 250 004, Uttar Pradesh, India

*Correspondence email - vijaimalik1973@gmail.com, amanmahavan1995@gmail.com

Received: 01 April 2025; Accepted: 02 September 2025; Available online: Version 1.0: 31 October 2025

Cite this article: Aman A, Deepti T, Vivek K, Pooja J, Bhanu A, Ashish K, Yeshvandra V, Vijai M. Molecular docking and dynamic simulation studies against the ERα of breast cancer using biomolecules from *Asparagus aethiopicus* L. Plant Science Today (Early Access). https:/doi.org/10.14719/pst.8614

Abstract

Globally, breast cancer is the major cause of mortality among women, with a significant proportion of cases associated with estrogen receptor alpha (ERα)-positive subtypes. Targeting ERα has emerged as a promising therapeutic strategy for effective management of breast cancer. This study explores the anticancer potential of bioactive secondary metabolites from the root tubers of *Asparagus aethiopicus* L. against ERα using a comprehensive *in silico* approach. Gas Chromatography-Mass Spectrometry (GC-MS) has been utilized to analyze the methanolic extracts of the root tubers. A total of 25 different phytochemicals were screened initially for drug likeness property using Lipinski's rule of five. Out of eight phytomolecules were selected based on their pharmacokinetic and absorption, distribution, metabolism, excretion and toxicity (ADMET) profiles. Further, six molecules were subjected for molecular docking analysis to assess binding affinity against ERα followed by Molecular Dynamics (MD) simulations, binding free energy (ΔG) calculations, Molecular Mechanics Poisson-Boltzmann Surface Area (MMPBSA) and PCA analysis. Drug-likeness assessments based on Lipinski's rule identified Pent-3-ene-2-one, 3-phenyl-oxime, Hydroperoxide1-methylbutyl and 4-Hydroxy-2-butanone as promising drug candidates. Molecular docking studies revealed strong interactions with the active site of ERα, whose binding energies vary from -3.8 to -7.3 kcal/mol. These 3 phytomolecules form stable hydrogen bonds with the critical residues of active sides of ERα viz. Glu353, Leu387, Arg394 and Lys449. The structural stability and minimal conformational alterations of ERα with ligand binding was confirmed by MD simulations. The stability of the protein-ligand complexes was supported by Root Mean Square Deviation (RMSD) with minimal deviation in RMSD (<0.6 nm), Root Mean Square Fluctuation (RMSF), Radius of Gyration (Rg) and with Solvent Accessible Surface Area (SASA) which indicates stable protein compactness. Moreover, PCA revealed dominant motions with minimal fluctuation in PC3, suggesting highly stabilized complexes. Hydrogen bond analysis highlighted stable and optimal interaction throughout the simulation. Among the tested compounds, Pent-3-ene-2-one, 3-phenyl-oxime exhibited the lowest binding free energy. This is primarily driven by Vander Waals interactions and polar solvation energy, indicating superior binding affinity. Thus, these finding explains the potential of *A. aethiopicus* phytochemicals as potent ERα inhibitors and provide a base for future *in vitro* and *in vivo* investigation into their application in breast cancer therapy.

Keywords: *A. aethiopicus*; breast cancer (Bc_a); ERα; molecular docking; MD simulation; MMPBSA; PCA

Introduction

Cancer is an unorganized and uncontrolled growth, in which controlling and regulating power have disappeared, leading to cell immortality and aggressive proliferation. These cancerous cells can invade surrounding tissues, exhibit metastatic behavior and spread to various organs. It is a major global health burden. It causes major economic losses and premature deaths across the world (1). Among women worldwide, breast cancer ranks as one of the most prevalent cancer, significantly contributing to global disease burden (2-4). In India, breast cancer accounts for over 27 % of all cancer cases, often resulting in disruption of normal mammary epithelial cell function (5). More than 60-70 % of breast cancer cases are identified as estrogen receptor alpha (ERα) positive subtypes (6-8). ERα is a hormone receptor which consists of 595 amino acids. It plays a vital role in gene transcription through of its two domains viz ligand-independent AF-1 and ligand-dependent AF-2. The receptor is also characterized by a DNA-binding domain (DBD) and a ligand-binding domain, connected by a hinge region (9-11). Within the nucleus, ligand bounded ERα undergoes conformational changes, recruits co-activators and directly interacts with specific DNA sequences called estrogen response elements (EREs). The latter is present in the promoter regions of target genes (12, 13).

Estrogen receptor (ER) exists in two isoforms, ERα and

ERß, which differ in activity, energy requirements, gene regulation and tissue distribution. Elevated estrogen levels can increase breast cancer risk by binding to ER, regulating apoptosis and promoting malignant cell growth (14). ERα is critical in breast cancer prevention and treatment, as it regulates differentiation and cell proliferation through paracrine signaling mechanism (15).

Asparagus aethiopicus L. (Asparagaceae) is a perennial monocot herb. It is grown both as indoor as well as outdoor plant. It has green aerial scrambling, twining, or arching stems with flattened cladophyll. The flowers are bisexual and pedicels are 5-8 mm. The inflorescence is axillary raceme. The fruit is berry which is red in color. Despite its broad horticultural presence, its potential therapeutic applications, particularly in breast cancer, remain unexplored.

Gas Chromatography-Mass Spectrometry (GC-MS) serves as a robust analytical tool for deciphering the complex chemical profiles of plant extracts, allowing for the identification of a diverse array of bioactive compounds. The secondary metabolites play an important role in conferring therapeutic properties (16-18). People are using plants for therapeutic purposes to reduce pain and discomfort and to expand their overall well-being since long back (19). The present study aims to identify bioactive compounds in the methanolic root tuber extract of *A. aethiopicus* through GC-MS analysis and assess their potential as inhibitors of ERα. A comprehensive literature review reveals a substantial body of work on molecular docking studies involving *Asparagus racemosus* and *Asparagus officinalis (*20-23*)*, but no similar studies have been conducted on *A. aethiopicus*. This evaluation includes drug-likeness characteristics, molecular docking, MD simulations, PCA and analysis of MMPBSA free energy. Moreover, it highlights a significant research gap, making this study the first to investigate the molecular docking and therapeutic potential of *A. aethiopicus* phytochemicals in the reference to breast cancer. *A. aethiopicus* act as a novel candidate for therapy of breast cancer. This research also helps in fulfilling an urgent need for safer, cost-effective treatments, for breast cancer management.

Methodology

Collection of plant material

The root tubers of *A. aethiopicus* were procured in October, 2024 from the Botanical Garden of CCS University, Meerut, Uttar Pradesh, India. Identification of the plant material was conducted through detailed morphological studies using relevant literature (24, 25). Voucher specimens were prepared and deposited in the herbarium and museum of the Botany department of CCS University, Meerut.

Preparation of plant extracts

Fifty grams fresh materials of root tubers were air-dried under room temperature for two weeks. The air-dried tubers were then ground into a fine powder using a mortar and pestle which weighed approximately 7 g. This fine ground powder was found in the ratio of 7.1:1 fresh-to-powder respectively. For extraction, around 1 g of the powdered sample was subjected to Soxhlet extraction using methanol as the solvent. The crude methanolic extract, enriched with bioactive compounds, was obtained through this process.

Gas Chromatography-Mass Spectrometry (GC-MS) analysis

The methanolic root tuber extract was analyzed using Gas Chromatography-Mass Spectrometry (GC-MS) to identify and quantify their chemical constituents. The analysis was performed on a high-resolution GC-MS system equipped with a SH-Rxi-5Sil MS column (30 m × 0.25 mm i.d., 0.25 µm film thickness), composed of 5 % biphenyl and 95 % dimethyl polysiloxane. The GC-MS conditions were as follows: column temperature (initially set as 50 °C and increased to 300 °C at a rate of 5 °C/min); Carrier Gas [Helium (He), at a constant flow rate of 1.0 mL/min]; Injection Volume (1 µL); Temperature Range (320-350 °C for the analysis) and Mass Detection Range [mass-to-charge ratio (m/z) 50-650]. The chemical constituents were identified based on their retention times and mass spectra (Fig. 1). An integrated chemical library search program was utilized for compound identification. Quantification of the relative abundance of each compound was

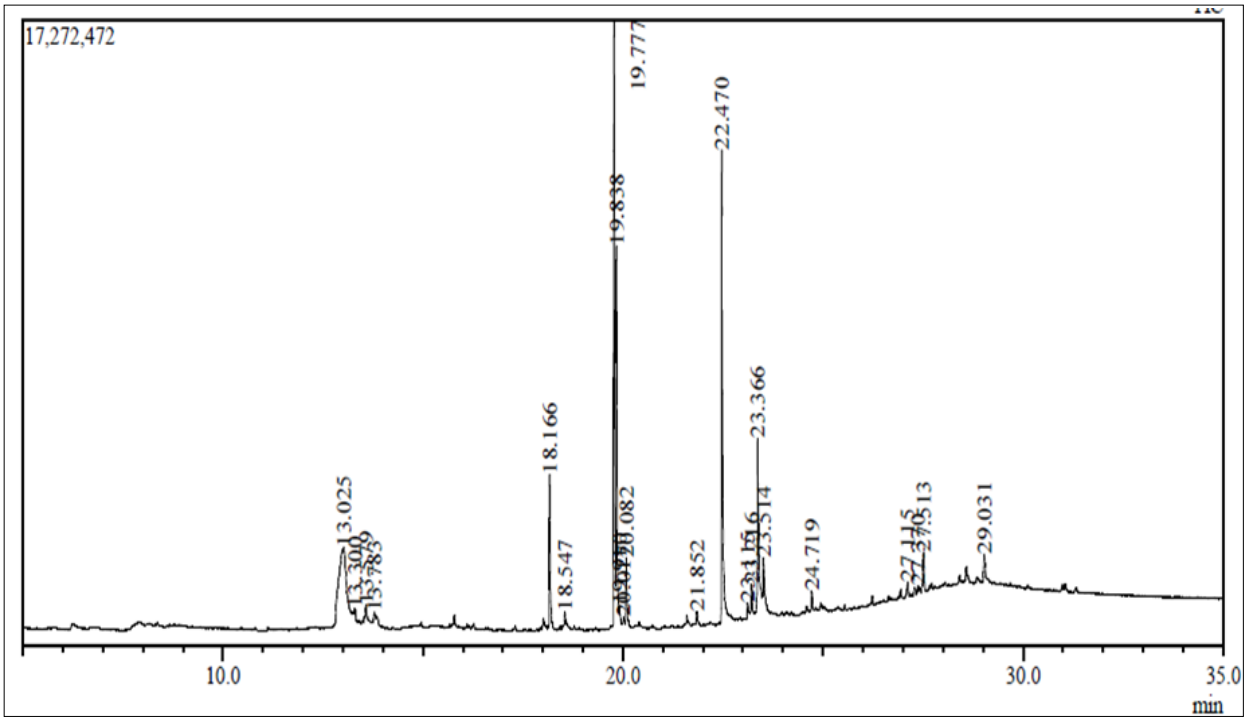

Fig. 1. GC-MS chromatogram showing the phytochemical profile of the methanolic root extract of *A. aethiopicus*.

performed through peak integration and area normalization. Thus, the result provides a comprehensive chemical profile of the plant extracts (Table 1) for identification of key bioactive compounds for further studies.

Molecular docking

Library generation and protein retrieval

Preparation of ligands: A total of 25 metabolites were identified through GC-MS analysis of the methanolic extract of *A. aethiopicus* root tubers. A library of eight structurally distinct phytomolecules were selected for molecular docking studies based on their bioactive potential. The 3D structures in SDF format of these compounds were retrieved from the Pub-Chem database (26). The SDF format was converted to PDBQT format (27).

Preparation of the target protein: The crystal structure of the target protein known as ERα, was retrieved from the RCSB Protein Data Bank (PDB ID: 3ERT) in PDB format (28). Protein preparation involved conversion to PDBQT format using AutoDock 4.2 (29). Energy minimization and structural optimization were performed using Swiss-PdbViewer (SPDBV) to ensure stability and suitability for docking simulations.

Procedure for molecular docking: Molecular docking was conducted using AutoDock Vina (29). The prepared protein and ligand library were evaluated for the binding affinities and interactions between the selected phytomolecules and the target enzyme.

Prediction of ADMET and physiochemical property: The ADMET, physiochemical, pharmacokinetic and toxicological properties of the selected compounds were evaluated using the Swiss-ADME online web server. Key parameters such as Blood-Brain Barrier (BBB) permeability; Human Intestinal Absorption (HIA); $CaCO_2$ permeability and drug clearance (9CL), were evaluated. Additionally, physicochemical properties including molecular weight, hydrogen bond donors/acceptors, lipophilicity, molar refractivity, rotatable bonds and overall drug-likeness were examined (30).

Molecular docking studies: AutoDock Vina was utilized for molecular docking to identify potential anticancerous compounds (31). The grid center coordinates were set to X = 24.447, Y = -1.464 and Z = 27.009, with a grid box size of 40 Å × 40 Å × 40 Å. Binding energy values ranged from -3.8 to -7.3 kcal/mol, indicating strong interactions between the phytomolecules and ERα.

Molecular dynamics simulations for assessing phytomolecule -protein complexes

MD simulations were carried out to assess the dynamic behavior of the protein-ligand complexes. Simulations utilized the AMBER force field (32) inbuilt in the GROMACS 2020.1-1 (33). The Acpype server (34) was utilized to generate topology file of the ligand. A cubic simulation box was used to solvate the protein-ligand complexes, followed by the addition of sufficient ions for neutralization of the system. Energy minimization was performed by employing the steepest descent algorithm, with a convergence threshold of less than 1000 kJ/mol/nm to eliminate any steric clashes within the system. Following energy minimization, equilibration was conducted in two phases:

a. **NVT equilibration**: A constant number, volume and temperature (NVT) simulation was carried out for 100 ns at 300 K, during which the system's coordinates were saved.

b. **NPT equilibration**: After achieving temperature stability, a constant number, pressure and temperature (NPT) simulation was conducted for an additional 100 ns. During this phase, the temperature and pressure were maintained at 300 K and 1 bar respectively, using coupling constants of 0.1 ps for both parameters.

In the NVT ensemble, the solvent and ions were kept unrestrained during the 100 ns equilibration. In the NPT ensemble, restraints on the protein and protein-ligand complexes were gradually reduced over the simulation duration to achieve a relaxed state. Hydrogen bonds were constrained using the LINCS algorithm (35). To ensure system stability at 300 K and 1 atm, temperature and pressure regulation were performed using Berendsen's thermostat and Parrinello-Rahman barostat respectively (36). The MD simulation trajectories were analyzed using tools available in the GROMACS package and custom Python 3.8 scripts. This computational framework

Table 1. Secondary metabolites identified in the root tubers of *A. aethiopicus* by GC-MS

Peak#	R.Time	Area	Area%	Height	Height %	Name	Base m/z
1	2.53	8651148	4.6	1194780	1.72	Hydroperoxide, 1-methylbutyl	43.05
2	2.661	10666393	5.68	1500412	2.16	Trimethylsilyl ethaneperoxoate	91
3	2.987	25553863	13.6	4790157	6.91	4-Hydroxy-2-Butanone	43.05
4	13.025	28214428	15.01	2087313	3.01	2-(Isobutoxymethyl)oxirane	57.05
5	13.3	1614671	0.86	366782	0.53	Dodecane, 4,6-dimethyl-	71.1
6	13.579	804328	0.43	411438	0.59	2,4-Di-tert-butylphenol	191.1
7	13.783	1416629	0.75	292891	0.42	Dodecanoic acid, methyl ester	74.05
8	18.166	7037594	3.74	4230739	6.1	Hexadecanoic acid, methyl ester	74.05
9	18.547	1000567	0.53	406298	0.59	n-Hexadecanoic acid	73
10	19.777	26928038	14.33	16737458	24.14	9,12-Octadecadienoic acid (Z,Z)-, methyl ester	67.05
11	19.838	18039174	9.6	10494403	15.13	9-Octadecenoic acid, methyl ester	55.05
12	19.91	1499275	0.8	580564	0.84	11-Octadecenoic acid, methyl ester	55.05
13	20.017	662012	0.35	258758	0.37	Eicosane	71.05
14	20.082	3358278	1.79	1881506	2.71	Methyl stearate	74.05
15	21.852	777928	0.41	339876	0.49	Tridecanoic acid, 4,8,12-trimethyl-, methyl ester	178.95
16	22.47	23763858	12.64	13025353	18.78	Phenol, 4,4′-(3-ethenyl-1-propene-1,3-diyl)bis	107.05
17	23.115	1196565	0.64	439589	0.63	Trans-4,4′-Dimethoxy-beta-methylchalcone	282.05
18	23.216	2094036	1.11	907951	1.31	Heneicosane	57.05
19	23.366	12971277	6.9	4883235	7.04	Phenol, 4,4′-(3-ethenyl-1-propene-1,3-diyl)bis	252.05
20	23.514	4813810	2.56	1528317	2.2	Pent-3-ene-2-one, 3-phenyl-, oxime	282.05
21	24.719	870830	0.46	517000	0.75	Tetracontane	57.05
22	27.115	1158749	0.62	434781	0.63	Stigmasta-5,22-dien-3-ol, acetate, (3-β)	81.1
23	27.37	701722	0.37	208073	0.3	Cholesta-4,6-dien-3-ol, (3-β)	135.05
24	27.513	2343931	1.25	1085479	1.57	β-Sitosterol acetate	147.1
25	29.031	1795999	0.96	738337	1.06	γ-Sitosterol	43.05

enabled the thorough investigation of the structural and dynamic behavior of the protein-ligand complexes under simulated physiological conditions.

Calculation of free energy using molecular mechanics Poisson-Boltzmann surface area (MMPBSA)

The binding free energy and residue-specific contributions were computed employing the MMPBSA method. In this approach, the solvation energy (ΔGnpsolv) was calculated as the sum of the non-polar component based on SASA and the polar component (ΔGpsolv), derived from the Poisson-Boltzmann equation. The binding energy analysis was conducted over a 100 ns trajectory using the *gmmpbsa* module of GROMACS (37).

Principal component analysis (PCA)

The PCA was performed using the Galaxy server (38). Protein conformation is essential for its function, especially in preserving the structural stability necessary for binding sites. The covariance matrix helps in analyzing large-scale motions of enzyme-ligand complexes during simulations. PCA is widely used to assess key conformational variations and flexibility in these complexes. Thus, this computational workflow provides a detailed evaluation of the structural and energetic features of the protein-ligand complexes for investigating into the therapeutic potential of *A. aethiopicus* phytochemicals.

Results

Drug-likeness properties

From a pool of 25 selected secondary metabolites, only eight molecules were identified to follow the Lipinski's rule of five (Supplementary Table S1) (39). These eight compounds were selected for further molecular docking studies. The secondary metabolites, along with their PubChem compound ID, molecular weight, molecular formula and canonical SMILES, are given in Table 2.

Analysis of molecular docking

Among the eight docked compounds, only six compounds showed significant binding interactions with ERα (Table 3). The binding energy of these six phytomolecules with ERα ranges from -3.8 to -7.3 kcal/mol (Fig. 2). The binding energies of the compounds were as follows: 4-Hydroxy-2-butanone (-3.8 kcal/mol); Hydroperoxide,1-methylbutyl and 2-(isobutoxymethyl)oxirane (-4.5 kcal/mol); Pent-3-ene-2-one,3-phenyl-,oxime (-6.6 kcal/mol); 2,4-Di-tert-butylphenol (-7.2 kcal/mol) and Trans-4,4′-Dimethoxy-beta-methylchalcone (-7.3 kcal/mol) (Fig. 2). These molecules established interactions with the active site residues of ERα via hydrogen bonds (H-bonds), Vander Waals forces, π-π stacking, π-σ and interaction of π-alkyl. Interaction analysis highlighted that the molecules consistently interacted with Leu387, a critical residue in the active site of ERα.

Molecular docking visualization of ERα complex

The docking results were analyzed and visualized using a combination of PyMOL and Ligplot+ software. PyMOL enables the three-dimensional (3D) visualization of protein-ligand interactions (40), while Ligplot+ provides two-dimensional (2D) schematic molecular interactions (41). The LigPlot+ software automatically generates interaction between profiles showing hydrogen bonds and hydrophobic interactions between the ligand and ERα residues. A comprehensive analysis of 3D molecular interactions, as estimated from docking revealed critical bonding patterns contributing to the stability of these complexes (Fig. 3).

Table 2. Secondary metabolites library of *A. aethiopicus* and drug-likeness based on Lipinski's rule of five

PubChem CID	Secondary metabolite name	Molecular weight (in g/mol)	Molecular formula	Canonical SMILES
139664	Hydroperoxide,1-methylbutyl (L2)	104.15	$C_5H_{12}O_2$	CCCC(C)OO
12571375	Trimethylsilyl ethaneperoxoate	148.23	$C_5H_{12}O_3Si$	CC(=O)OO[Si](C)(C)C
111509	4-Hydroxy-2-butanone (L3)	88.11	$C_4H_8O_2$	CC(=O)CCO
98155	2-(Isobutoxymethyl)oxirane	130.18	$C_7H_{14}O_2$	CC(C)COCC1CO1
7311	2,4-Di-tert-butylphenol	206.32	$C_{14}H_{22}O$	CC(C)(C)C1=CC(=C(C=C1)O)C(C)(C)C
6915833	Nyasol	252.31	$C_{17}H_{16}O_2$	C=C[C@H](/C=C\C1=CC=C(C=C1)O)C2=CC=C(C=C2)O
5337676	trans-4,4′-Dimethoxy-beta-methylchalcone	282.30	$C_{18}H_{18}O_3$	C/C(=C\C(=O)C1=CC=C(C=C1)OC)/C2=CC=C(C=C2)OC
9602655	Pent-3-ene-2-one, 3-phenyl-, oxime (L1)	175.23	$C_{11}H_{13}NO$	C/C=C(\C1=CC=CC=C1)/C(=N/O)/C

Note: L1 = Pent-3-ene-2-one, 3-phenyl-, oxime; L2 = Hydroperoxide,1-methylbutyl; L3 = 4-Hydroxy-2-butanone.

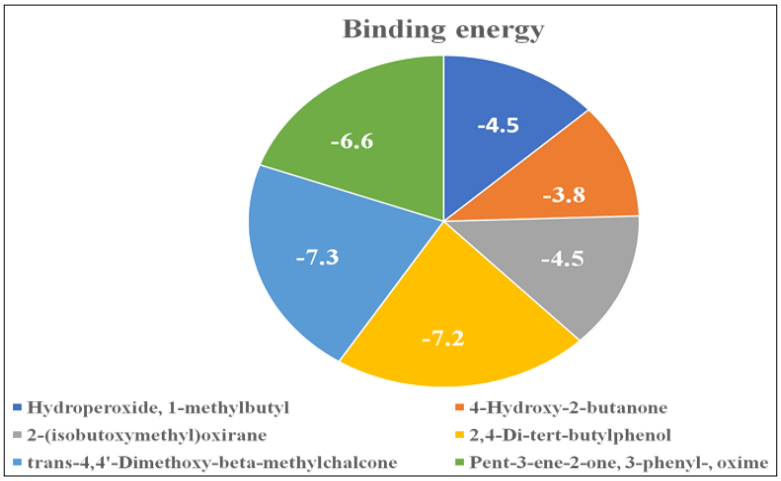

Fig. 2. Binding energies of selected secondary metabolites of *A. aethiopicus* against ERα as determined by molecular docking.

Table 3. Top-docked secondary metabolites of *A. aethiopicus* against ERα

Sr. No.	Compounds name	Type of bond interaction	Number of Bonds	Bond formation (amino acids and ligands)
1	Hydroperoxide,1methylbutyl	π-alkyl	5	Leu391, Leu387, Met388, Phe404, Leu346
		Hydrogen bond	2	Arg394, Leu387
2	4-Hydroxy-2-butanone	Hydrogen bond	2	Lys449, Glu353
3	2-(Isobutoxymethyl)oxirane	Hydrogen bond	1	Lys449
		Carbon-Hydrogen bond	1	Glu355
		Alkyl bond	3	Met357, Pro324, Ile386
4	2,4-Di-tert-butylphenol	π-sulfur	1	Met421
		π-alkyl	3	Leu346, Leu525, Leu384
5	trans-4,4′-Dimethoxy-beta-methylchalcone	π-alkyl	7	Ala350, Leu525, Met343, Leu346, Leu387, Leu391, Phe404
6	Pent-3-ene-2-one, 3-phenyl-oxime	Hydrogen Bond	3	Glu353, Leu387, Arg394
		π-sulfur	2	Met421, Met388
		π-alkyl	6	Leu391, Leu387, Leu346, Ala350, Leu349, Phe404

Molecular dynamics simulations

Additionally, MD simulations of certain phytomolecules were carried out. Proteins can experience a wide variety of conformational changes as a result of ligand interaction. Therefore, we have calculated several metrics such as RMSD, RMSF and Rg for free and all protein-ligand complexes in order to analyse the structural changes induced by ligand in protein and the stability of protein-ligand complexes (Table 4).

Root Mean Square Deviation (RMSD) analysis

The RMSD is an important parameter to quantify the extent of conformational changes in proteins during MD simulations. In this study, the RMSD of the Cα atoms from their initial structures were calculated to evaluate the stability of the protein-ligand complexes. The time-dependent RMSD of the backbone atoms of ERα in both free and ligand-bounded state was observed to range between 0.20 and 0.60 nm, stabilizing to a plateau within 20 ns of the simulation. These low RMSD values suggest a high degree of stability for ERα in both its free and ligand-bound conformations. Notably, the RMSD values for all systems remained below 0.6 nm throughout the simulation period (Fig. 4A). This indicates minimum deviation of the enzyme from its starting conformation. Furthermore, the binding of phytomolecules did not induce significant conformational changes in the protein backbone. This affirms the structural stability of ERα in the presence of ligands.

Flexibility and dynamics analysis using RMSF

The flexibility and dynamics of the system were evaluated through RMSF analysis. Most of the enzyme residues exhibited RMSF values that vary from 0.15 to 0.19 nm (Fig. 4B). This observation with minimum fluctuations suggests that the positional stability of the amino acid residues remains largely unaffected by the binding of phytochemicals to the active site of ERα. Consequently, it can be concluded that the ligand-protein interactions does not significantly alter the overall dynamics of protein.

Radius of gyration analysis

The Rg serves as a measure of protein compactness, with lower Rg values indicating greater stability. Since, ligand binding can potentially induce protein unfolding and the variation in Rg was analyzed throughout the simulation for all cases. For the unbound ERα the Rg values were centered around ~1.85 nm. Similarly, Rg values varying from ~1.85 to 1.92 nm were observed for ERα bound to the proposed phytomolecules (Fig. 4C). These results indicate that the binding of the phytomolecules does not affect the structural integrity or compactness of ERα.

Solvent Accessible Surface Area (SASA) analysis

Hydrophobic interactions displayed between non-polar amino acids play an important role in stabilizing globular proteins by shielding these residues within hydrophobic cores from the aqueous environment. The SASA provides a theoretical measure of changes in protein accessibility to solvent that reflects the role of free energy of solvation for each atom in the system, including water and the polar and non-polar amino acids of the protein. In the case of independent ERα, the SASA profile peaked at approximately ~130 nm^2. Upon binding with ligands, SASA values shifted to a range of ~132-138 nm^2 (Fig. 4D). Since the observed SASA values show minimal deviation compared to the control, it can be inferred that the binding of these compounds does not disrupt protein folding or alter the structural integrity of ERα.

Hydrogen bond analysis

The H-bond interactions between ERα and the bioactive metabolites were evaluated using the hydrogen bond module of GROMACS. The distribution of H-bonds was monitored throughout the 100 ns simulation, with the maximum H-bond distances ranging from 0.25 to 0.35 nm. The H-bond distribution graph (Fig. 4F) indicates that H-bond formation initiated at a distance of 0.25 nm between the H-bond donor and acceptor, with the maximum distribution observed at a distance of 0.30 nm. Thus, these findings highlight the stability and optimal geometry of hydrogen bond interactions (Fig. 4E) in the ligand-receptor complexes.

Binding free energy analysis

The binding free energy (ΔG) of the ligand-ERα complexes were calculated using MMPBSA analysis. This provides insights into the binding potential of ligands. The MMPBSA results confirmed that all tested molecules successfully bind to the active site of ERα to

Table 4. Average values of different parameters of MD simulations for L1, L2 and L3 against ER-α

Sr. no.	Parameters	Control	L1	L2	L3
1	Backbone RMSD	0.328 ± 0.0313	0.267 ± 0.036	0.239 ± 0.021	0.272 ± 0.030
2	Complex RMSD	-	0.620 ± 0.0661	0.273 ± 0.035	0.340 ± 0.030
3	Ligand RMSD	-	0.079 ± 0.018	0.082 ± 0.017	0.070 ± 0.015
4	Radius of gyration	1.586 ± 0.180	1.592 ± 0.177	1.581 ± 0.173	1.584 ± 0.172
5	SASA	133.438 ± 4.394	134.850 ± 3.887	133.236 ± 2.737	135.263 ± 3.025
6	RMSF	0.125 ± 0.101	0.128 ± 0.098	0.119 ± 0.072	0.125 ± 0.092

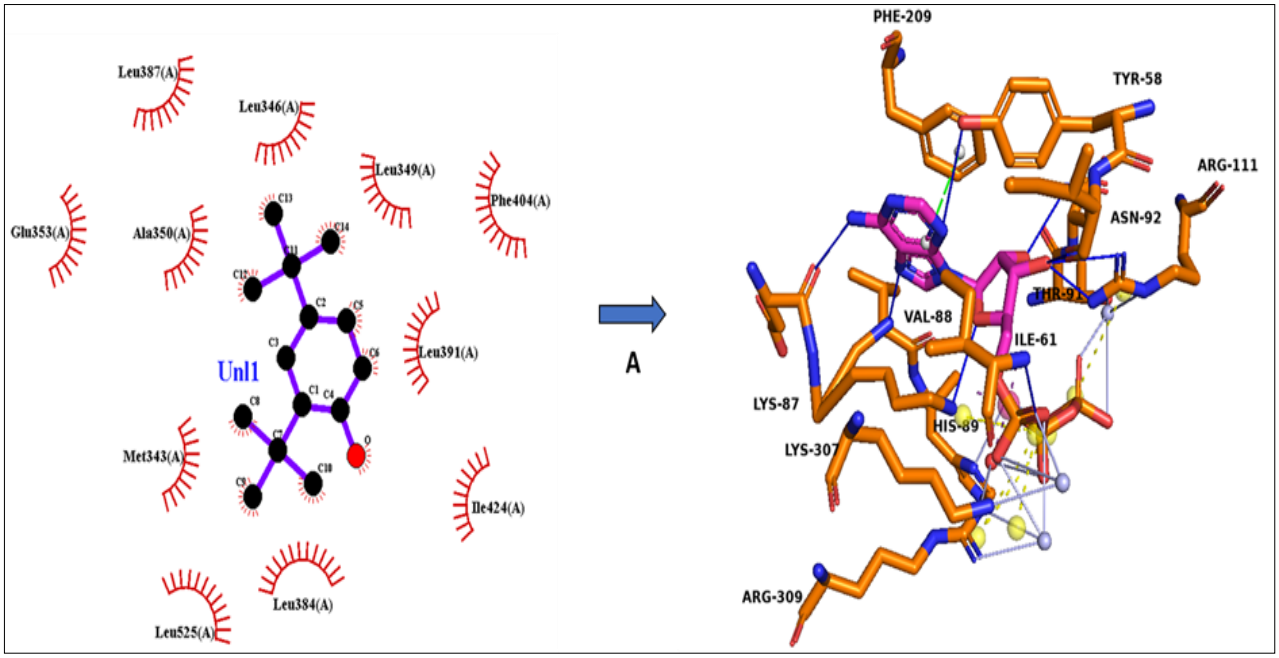
Leu387(A)
Leu346(A)
Leu349(A)
Phe404(A)
Glu353(A)
Ala350(A)
Unl1
Leu391(A)
Met343(A)
Ile424(A)
Leu384(A)
Leu525(A)
A
PHE-209
TYR-58
ARG-111
ASN-92
THR-91
VAL-88
ILE-61
LYS-87
HIS-89
LYS-307
ARG-309

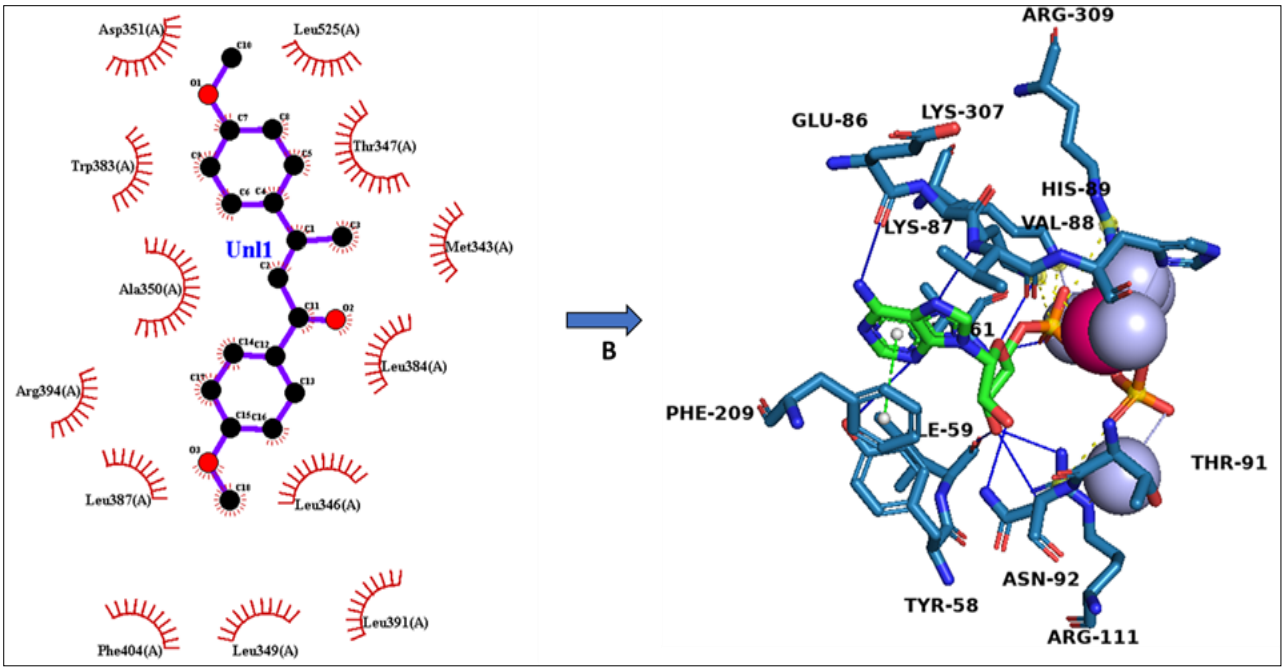
Asp351(A)
Leu525(A)
Trp383(A)
Thr347(A)
Unl1
Met343(A)
Ala350(A)
Leu384(A)
Arg394(A)
Leu387(A)
Leu346(A)
Phe404(A)
Leu349(A)
Leu391(A)
B
ARG-309
GLU-86
LYS-307
HIS-89
LYS-87
VAL-88
PHE-209
THR-91
ASN-92
TYR-58
ARG-111

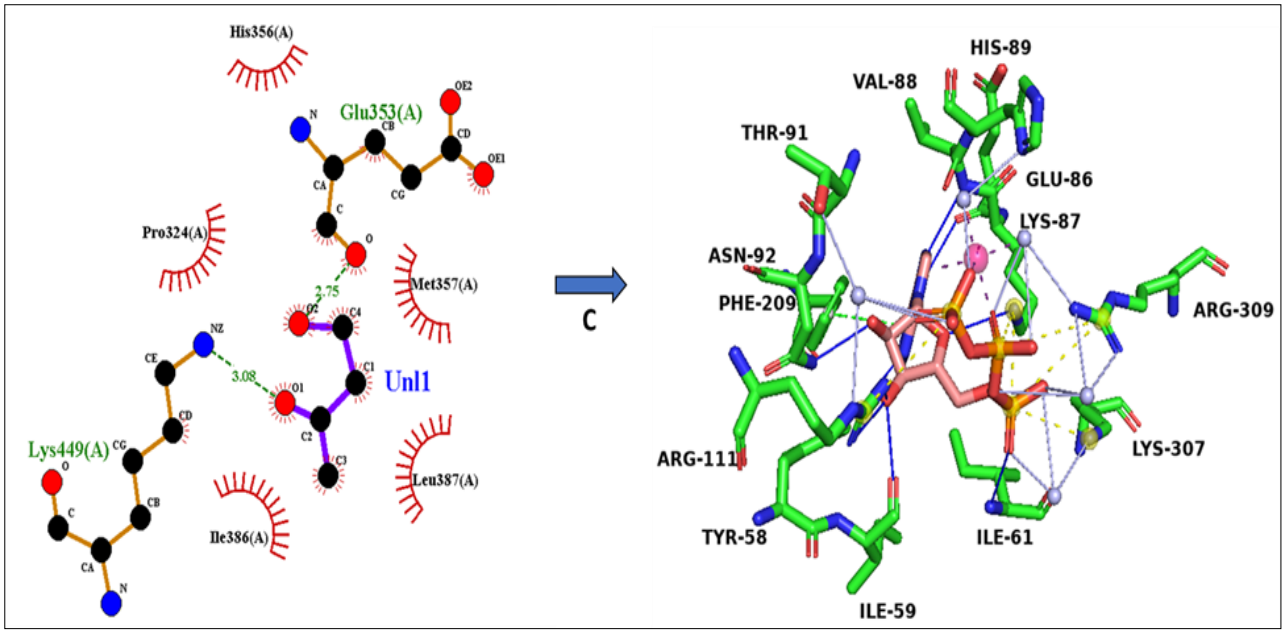
His356(A)
Glu353(A)
Pro324(A)
Met357(A)
2.75
3.08
Unl1
Lys449(A)
Leu387(A)
Ile386(A)
C
HIS-89
VAL-88
THR-91
GLU-86
LYS-87
ASN-92
PHE-209
ARG-309
LYS-307
ARG-111
TYR-58
ILE-61
ILE-59

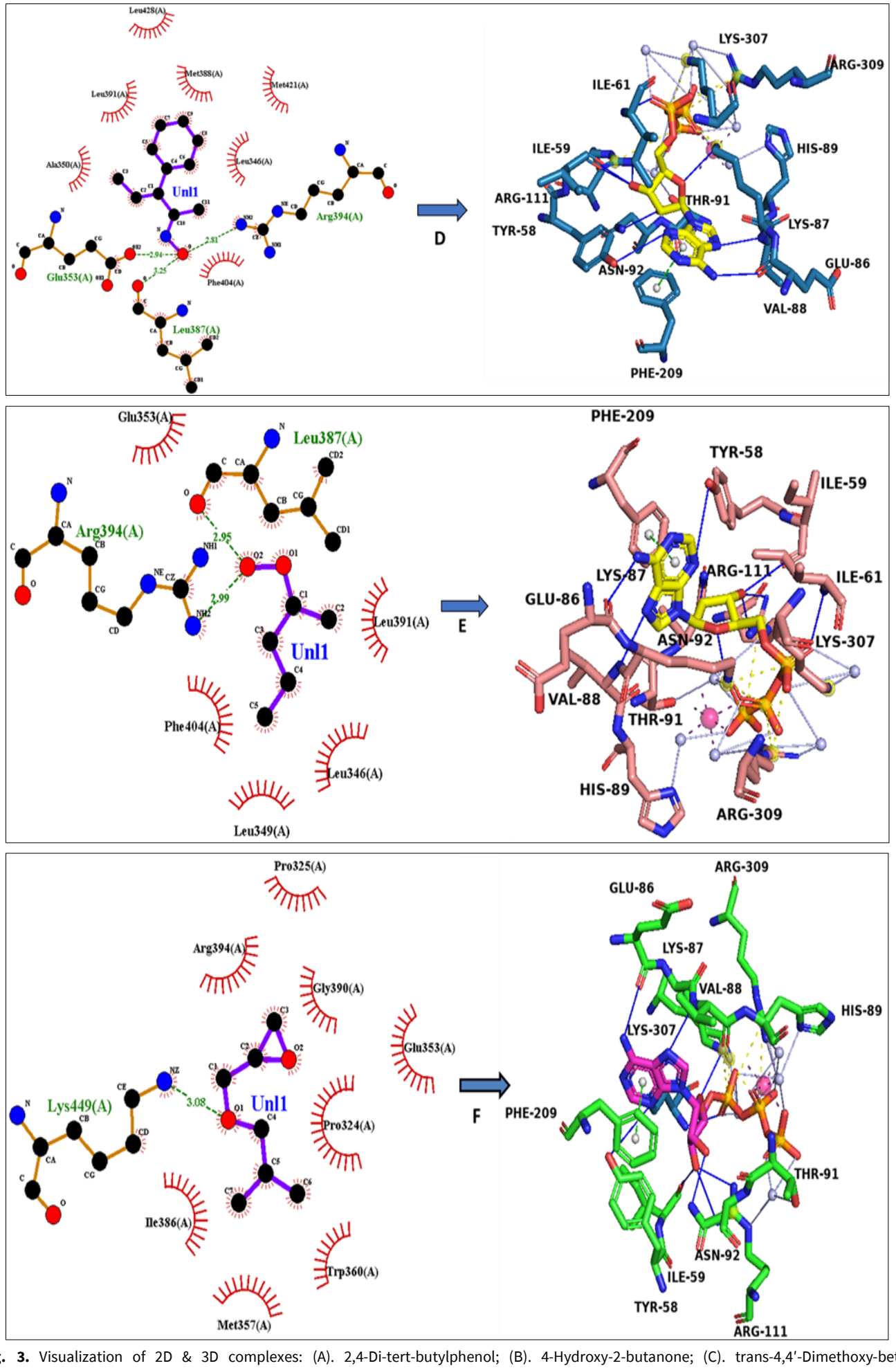

Fig. 3. Visualization of 2D & 3D complexes: (A). 2,4-Di-tert-butylphenol; (B). 4-Hydroxy-2-butanone; (C). trans-4,4′-Dimethoxy-beta-methylchalcone; (D). Pent-3-ene-2-one, 3-phenyl-, oxime; (E). Hydroperoxide, 1-methylbutyl, genistein; (F). 2-(isobutoxymethyl) oxirane.

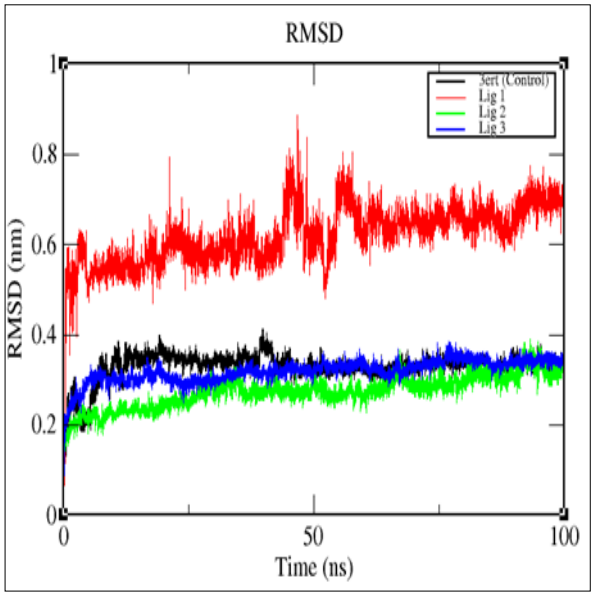

A

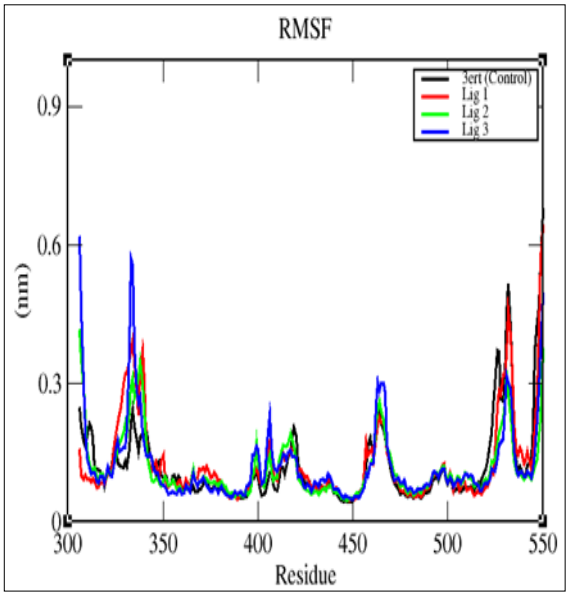

B

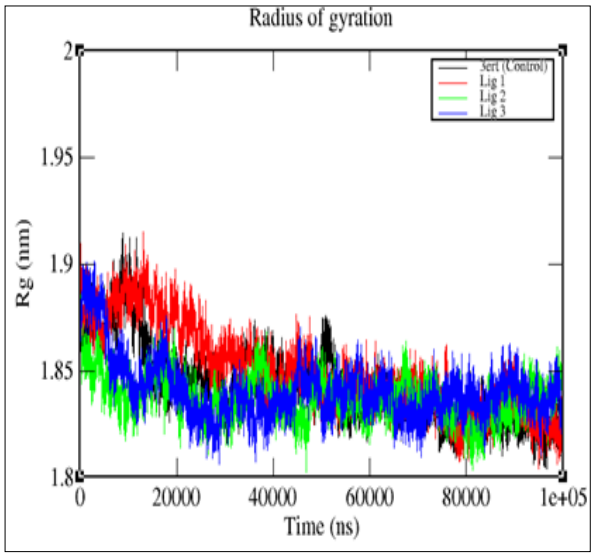

C

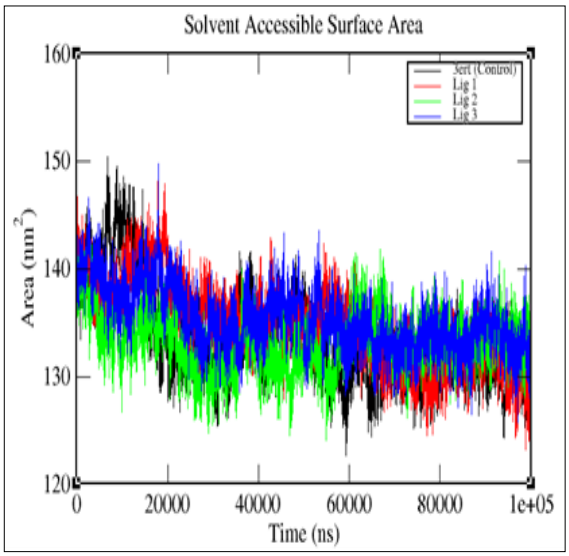

D

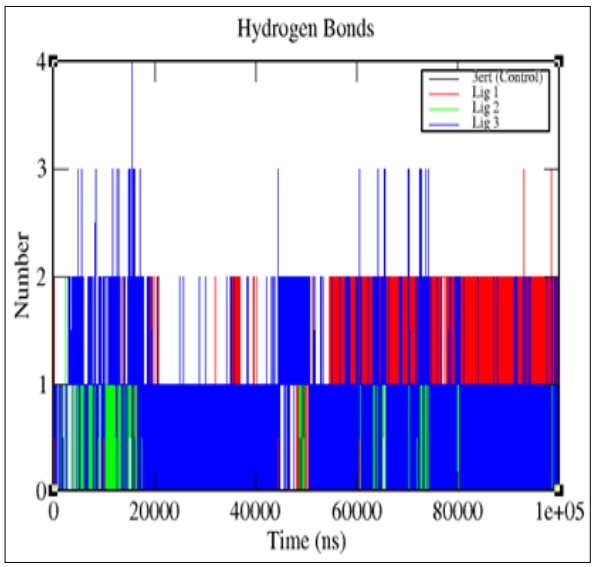

E

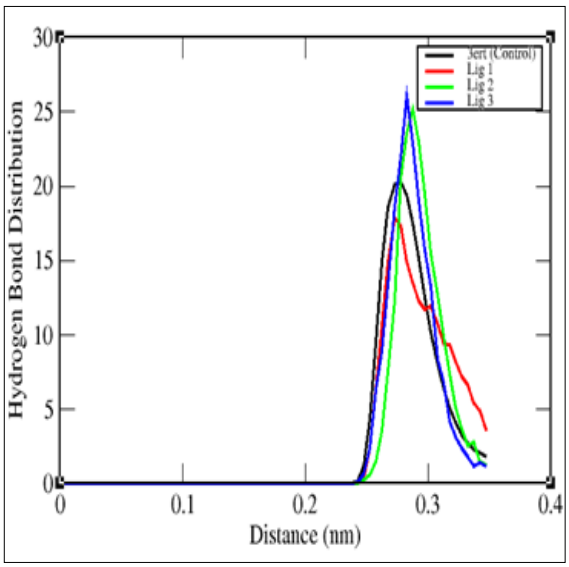

F

Fig. 4. Plot of MD simulation between L1, L2, L3 & ERα: (A) RMSD; (B) RMSF; (C) Radius of gyration; (D) SASA; (E) H-bond; (F) H-bond distribu-

form stable complexes. Among the three tested ligands, L1 exhibited the lowest binding free energy, indicating the highest binding affinity with ERα. The variation in ΔG values was primarily influenced by the Vander Waals interaction component (ΔEvdw) and the polar solvation free energy component (ΔGpsolv), which plays significant role in lowering the binding free energy (Fig. 5). Moreover, other additional energy components including, ΔEEL, ΔGpsolv and ΔGnpsolv. These energies also contributed to the overall binding free energy of the enzyme-ligand complexes (Table 5).

Principal component analysis (PCA)

PCA was utilized to determine the conformational changes in the protein due to binding of ligands (L1, L2 and L3) with protein. PCA reveals the collective motions of MD trajectories. The PC1, PC2 and PC3 are represented in Fig. 6(A-C). The eigenvalues of receptor for the first 20 modes of motion have been plotted against the respective eigenvector index. The conformational changes in all clusters are indicated by PCA. The blue region shows the most significant movements, while the white region shows intermediate movements and the red region shows the least flexible movement.

Table 5. Free energy depiction of protein ligand-complex (KJ/mol) through MMPBSA analysis

Sr. No.	Compound	$\Delta E_{VDWAALS}$	ΔE_{EL}	ΔE_{PB}	ΔE_{NPOLAR}	ΔG_{GAS}	ΔG_{SOLV}	ΔTotal
1	L1	-28.95 ± 1.68	-10.51 ± 3.15	21.26 ± 1.89	-2.72 ± 0.02	-39.47 ± 3.12	18.78 ± 1.87	-20.69 ± 1.77
2	L2	-15.24 ± 1.16	-15.90 ± 1.64	17.62 ± 1.07	-2.02 ± 0.035	-30.90 ± 1.24	15.60 ± 1.10	-15.30 ± 1.42
3	L3	-14 ± 1.63	-8.89 ± 6.14	22.23 ± 4.15	-1.70 ± 0.04	-22.89 ± 5.88	20.54 ± 4.19	-2.36 ± 1.91

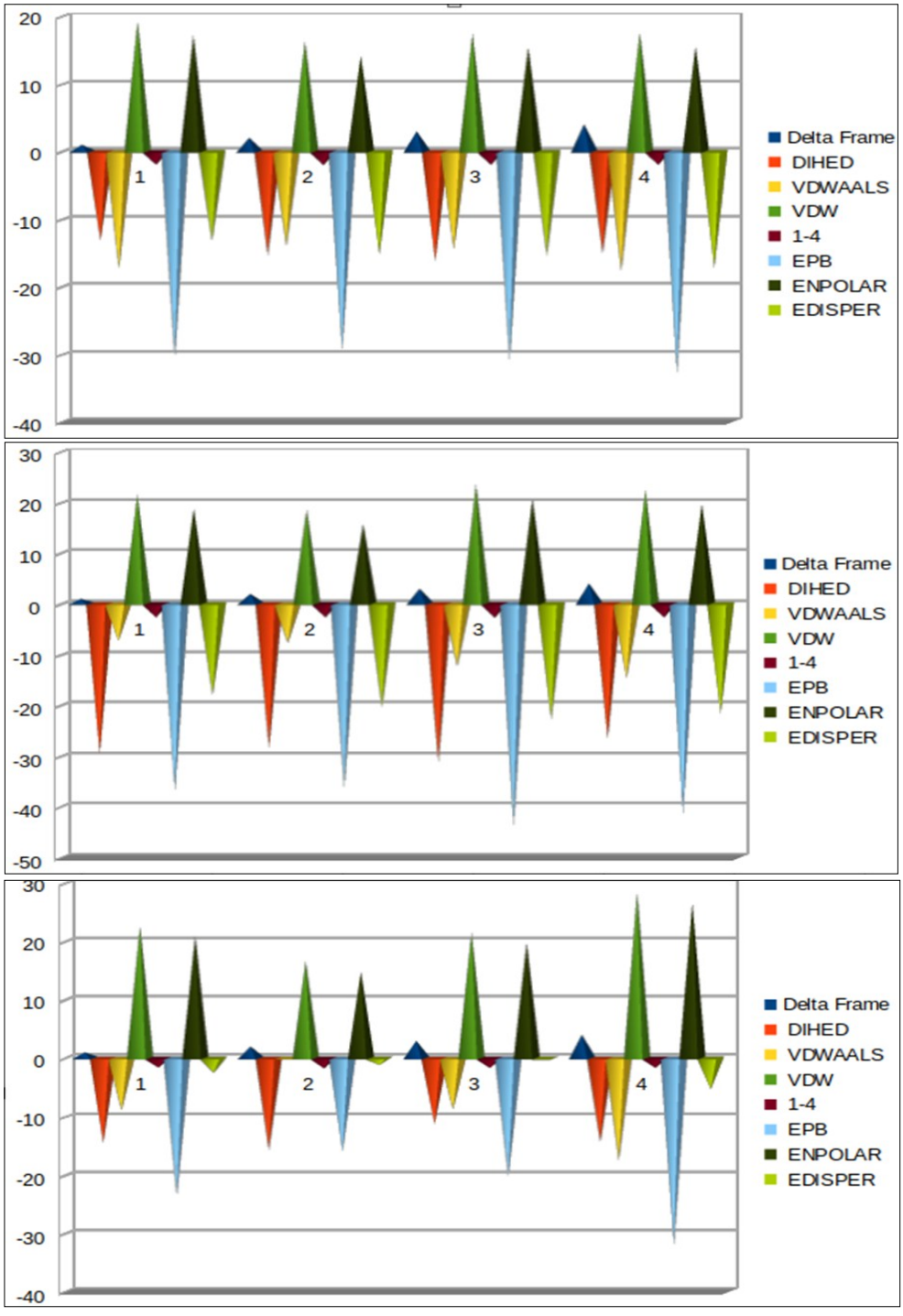

Fig. 5. Diagrammatic representation of protein-ligand complexes through MM-PBSA: (A) L1 & ERα; (B) L2 & ERα; (C) L3 & Erα.

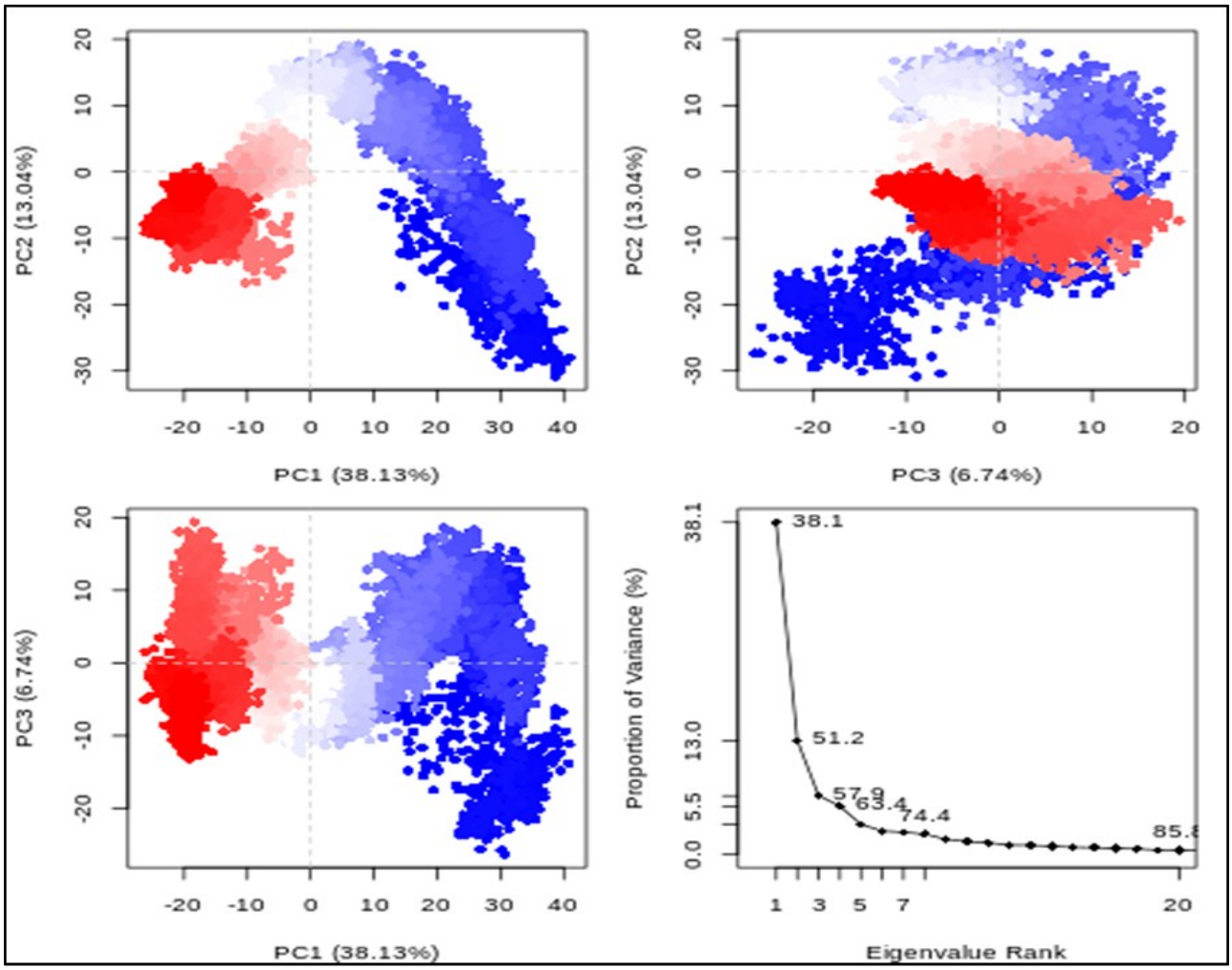
PC2 (13.04%)
PC1 (38.13%)
PC3 (6.74%)
PC1 (38.13%)
PC2 (13.04%)
PC3 (6.74%)
Proportion of Variance (%)
38.1
51.2
57.9
63.4
74.4
Eigenvalue Rank

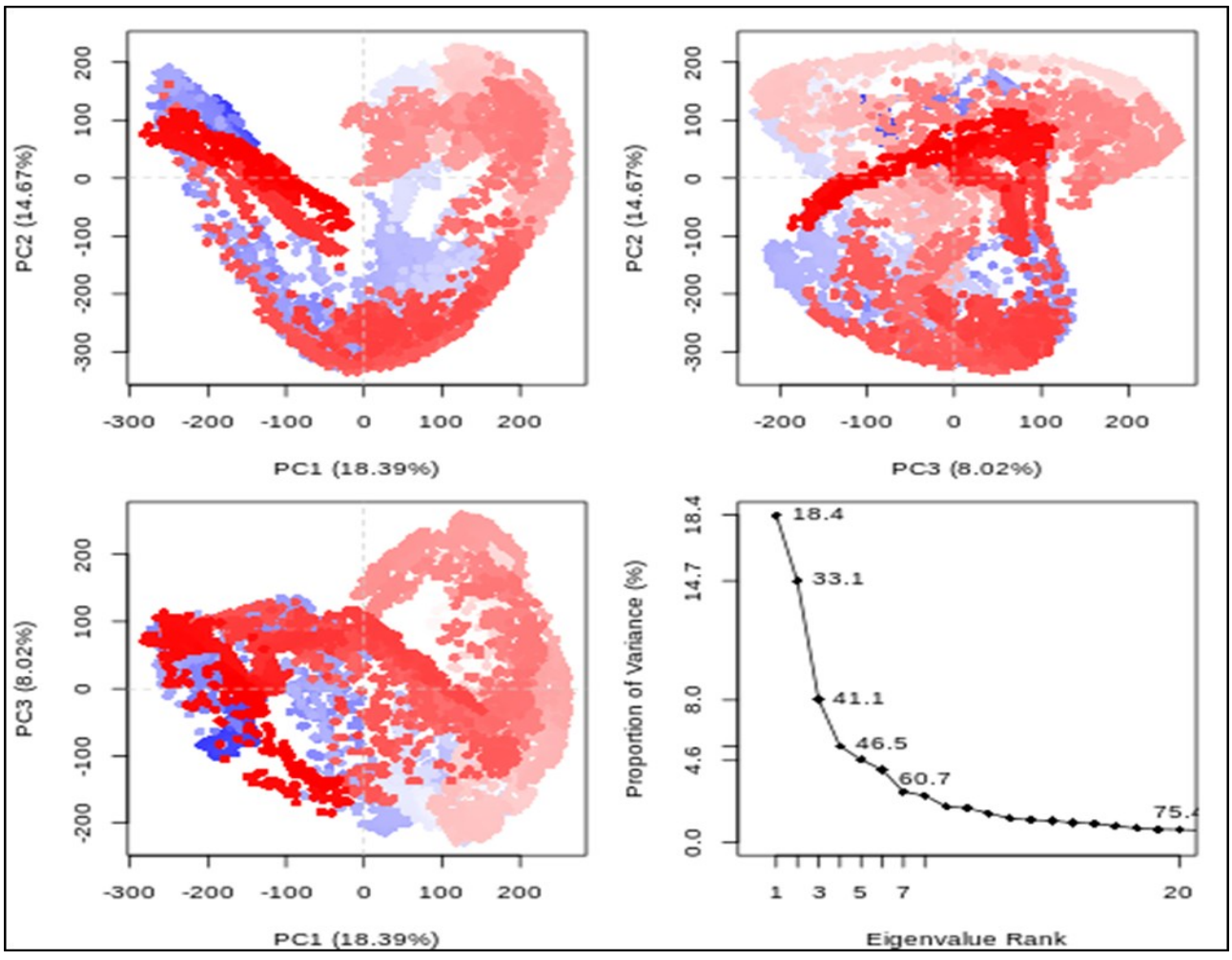
PC2 (14.67%)
PC1 (18.39%)
PC3 (8.02%)
PC1 (18.39%)
PC2 (14.67%)
PC3 (8.02%)
Proportion of Variance (%)
18.4
33.1
41.1
46.5
60.7
Eigenvalue Rank

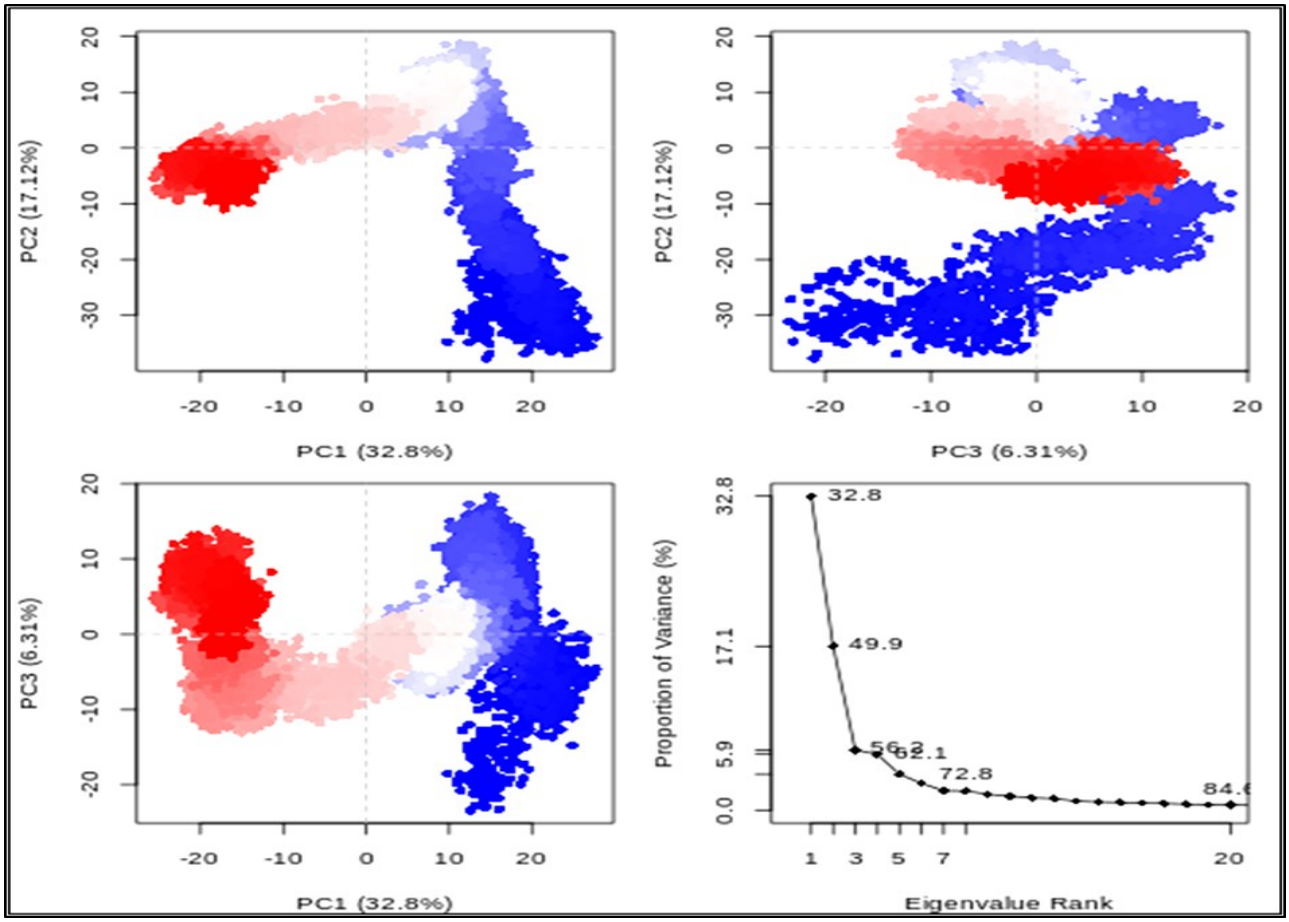

Fig. 6. (A-C) Interpretation of variance (ERα - L1, L2, L3) against eigenvalues calculated by principal component analysis.

Overall protein movement was controlled by higher value of eigenvectors. In our system the values of eigenvector were 0.0 to 38.1, 0.0 to 18.4 and 0.0 to 32.8 for L1, L2 and L3 respectively, whereas eigenvalue ranges from 38.1 % to 74.4 %, 18.4 % to 60.7 % and 32.8 % to 72.8 % for L1, L2 and L3 respectively. These higher values demonstrated the dominant movement of the protein. The PC1 cluster in PCA plot showed the highest variability of 38.13 %, 18.39 % and 32.8 %, PC2 showed variability of 13.04 %, 14.67 % and 17.12 %, while PC3 showed minimum variability of 6.74 %, 8.02 % and 6.31 %. The minimum variability of PC3 indicates highly stabilized protein ligand binding due to minimum fluctuations of values and a compact structure as compared to the PC1 and PC2 clusters.

Discussion

Molecular docking has emerged as a dispensable and high throughput *in silico* tool for identifying potential lead compounds against diverse molecular targets implicated in disease pathophysiology (42). Within the context of hormone-responsive cancers, ERα has long been recognized as a critical therapeutic target, particularly in estrogen-dependent breast cancers. A plethora of studies has evaluated the interaction of natural compounds with ERα and other proteins (49, 50), demonstrating the utility of phytochemicals as potential modulators with lesser side effects and improved biocompatibility. Several published literatures reflects a consistent interest in plant-derived molecules for anti-estrogenic activities. Compounds like Carvacrol from *Ocimum sanctum* (43), Isocorilagin from *Phyllanthus emblica* (44) and Anolignan B from *Terminalia bellerica* (45) have shown promising ERα inhibitory potential. Other important inhibitors include quercetin-3-α-arabinoside, Guajadial, psidial A, Stigmasterol and Daidzein, derived from various ethnomedicinal plants. This affirms the strategic use of phytoconstituents in hormone-receptor targeting (46-48). A comprehensive *in silico* exploration on *A. racemosus* (20) against ERα and related targets such as ERβ, HSP90 and 17β-HSD1 further supports the therapeutic promise of the genus *Asparagus* in endocrine malignancies. In addition to this, several species of *Asparagus* have been evaluated for pharmacological activities beyond oncology. For instance, *A. racemosus* has been studied for neurodegenerative diseases like Alzheimer's through interactions with AChE, BuChE, BACE1 and MAO-B (53) and *Asparagus africinus* for hormonal receptors like LH and FSH (54). Similarly, *A. officinalis* has been investigated against key cancer-associated targets including AKT1, IL-6, VEGFA, MYC and EGFR (55). This indicates the broad-spectrum bioactivity of genus *Asparagus*. Despite this expansive coverage, the phytoconstituents of *Asparagus aethiopicus* remain largely unexplored, particularly in the context of breast cancer and ERα modulation. Several previous studies have indicated its antiviral (52), antioxidant (56) and anthelminthic (57) properties, but there is a noticeable gap in cancer-related molecular studies involving ERα. Moreover, although modulators such as Lupeol, Genistein and 7-Hydroxy-2-Methylisoflavone have demonstrated ERα affinity (58), no reported evidence exists for similar activity from *A. aethiopicus*. Our study addresses this research void by being the first to utilize molecular docking and molecular dynamics (MD) simulations to evaluate the binding efficacy and conformational stability of *A. aethiopicus*-derived biomolecules with ERα. The findings provide valuable preliminary

insights that could pave the way for novel plant-based therapeutics in estrogen-dependent breast cancer. Additionally, the integration of dynamic simulation studies reinforces the docking outcomes, offering a more realistic appraisal of ligand-receptor interactions under physiological conditions.

Conclusion

In this study, the anticancer potential of bioactive metabolites from *A. aethiopicus* against ERα was investigated using an *in silico* approach. The molecular docking analysis revealed that six metabolite showed the binding affinity against ERα, with binding energies varying from -3.8 to-7.3 kcal/mol. The compounds 4 -Hydroxy - 2 - butanone Hydroperoxide, 1 - methylbutyl; 2 -(isobutoxymethyl)oxirane; Pent-3-ene-2-one,3 -phenyl-,oxime; 2, 4 - Di - tert - butylphenol and trans - 4, 4′ - Dimethoxy-beta-methylchalcone demonstrates the strongest binding interactions with ERα. The findings suggest that L1, L2 and L3 form hydrogen bond with critical residues of the ERα, such as (L1 - Glu353, Leu387, Arg394), (L2 - Arg394, Leu387) and (L3 - Lys449, Glu353). However, L1, L2 and L3 has not yet been reported as an anticancer compound. The MD simulations, PCA and MMPBSA free energy calculations further validated the stability and binding efficiency of L1, L2, L3 and ERα protein complex. L1, L2 and L3 from *A. aethiopicus* shows high binding scores and stability. This indicates that these molecules (L1, L2 and L3) potentially inhibit ERα which is essential for the treatment of breast cancer. Thus, the present study offers valuable insights for the phytochemicals extracted from roots of *A. aethiopicus* against cancer. Finally, this study not only opens new door for medicinal practitioners for experimental validation but also for pharmacologist for identification of its phytochemical therapeutics.

Limitations of the study

While this study highlights the potential interaction of *A. aethiopicus* phytochemical with ERα through computational approaches, it is primarily based on *in silico* analyses. Therefore, the findings need to be supported by experimental validation through *in vitro* and *in vivo* studies to confirm their biological activity and pharmacokinetic profiles.

Acknowledgements

The authors are grateful to Head, Department of Botany, Chaudhary Charan Singh University Meerut India for providing computational facilities and CSIR, New Delhi (India) for providing financial support.

Authors' contributions

AA contributed to writing the original draft and performed the *in silico* analysis. DT, PJ and BA provided resources. VK and AK carried out the *in silico* analysis. YV contributed to writing, reviewing and editing the manuscript. VM supervised the work and was involved in reviewing, writing and editing the manuscript. All authors read and approved the final manuscript.

Compliance with ethical standards

Conflict of interest: Authors do not have any conflict of interest to declare.

Ethical issues: None

References

1. Choudhir G, Kumar S, Kumar A. Targeting telomeric RNA quadruplexes with natural metabolites to prevent cancer. In silico Pharmacology. 2024;12:112. https://doi.org/10.1007/s40203-024-00283-4
2. Jemal A, Bray F, Center MM, Ferlay J, Ward E, Forman D. Global cancer statistics. CA: A Cancer Journal for Clinicians. 2011;61(2):69-90. https://doi.org/10.3322/caac.20107
3. Boyer JA, Gadal S, Rosen EY, Sharma M, Dorso MA, Maid N, et al. eIF4A controls translation of estrogen receptor alpha and is a therapeutic target in advanced breast cancer. Proceedings of the National Academy of Sciences. 2025;*122*(30):e2424286122. https://doi.org/10.1073/pnas.2424286122
4. Rugo HS, Rumble RB, Macrae E, Barton DL, Connolly HK, Dickler MN, et al. Endocrine therapy for hormone receptor-positive metastatic breast cancer: American Society of Clinical Oncology guideline. Journal of Clinical Oncology. 2016;*34*(25):3069-103. https://doi.org/10.1200/JCO.2016.67.1487
5. Torre LA, Bray F, Siegel R, Ferlay J, LortetⅧTieulent J, Jemal A. Global cancer statistics, 2012. CA: A Cancer Journal for Clinicians. 2015;65(2):87-108. https://doi.org/10.3322/caac.21262
6. Sahayarayan JJ, Rajan KS, Vidhyavathi R, Nachiappan M, Prabhu D, Alfarraj S, et al. *In-silico* protein-ligand docking studies against the estrogenprotein of breast cancer using pharmacophore based virtual screening approaches. Saudi Journal of Biological Sciences. 2021;28(1):400-7. https://doi.org/10.1016/j.sjbs.2020.10.023
7. Altwegg KA, Vadlamudi RK. Role of estrogen receptor coregulators in endocrine resistant breast cancer. Exploration of Targeted Anti-tumor Therapy. 2021;2:385-400. https://doi.org/10.37349/etat.2021.00052
8. Mangani S, Piperigkou Z, Karamanos NK, Koletsis NE, Ioannou P. Estrogen receptors and extracellular matrix: the critical interplay in cancer development and progression. The FEBS Journal. 2025;292(7):1558-72. https://doi.org/10.1111/febs.17270
9. Germain P, Staels B, Dacquet C, Spedding M, Laudet V. Overview of nomenclature of nuclear receptors. Pharmacological Reviews. 2006;58(4):685-704. https://doi.org/10.1124/pr.58.4.2
10. Kumar R, Zakharov MN, Khan SH, Miki R, Jang H, Toraldo G, et al. The dynamic structure of the estrogen receptor. Journal of Amino Acids. 2011;2011:812540. https://doi.org/10.4061/2011/812540
11. Ng HW, Perkins R, Tong W, Hong H. Versatility or promiscuity: The estrogen receptors, control of ligand selectivity and an update on subtype selective ligands. International Journal of Environmental Research and Public Health. 2014;11(9):8709-42. https://doi.org/10.3390/ijerph110908709
12. Kumar V, Chambon P. The estrogen receptor binds tightly to its responsive element as a ligand-induced homodimer. Cell. 1988;55(1):145-56. https://doi.org/10.1016/0092-8674(88)90017-7
13. Jakacka M, Ito M, Weiss J, Chien PY, Gehm BD, Jameson JL. Estrogen receptor binding to DNA is not required for its activity through the nonclassical AP1 pathway. The Journal of Biological Chemistry. 2001;276(17):13615-21. https://doi.org/10.1074/jbc.M008384200
14. Agabio R, Madeddu C, Contu P, Cosentino S, Deiana M, Massa E, et al. Alcohol consumption is a modifiable risk factor for breast cancer: are women aware of this relationship. Alcohol and Alcoholism. 2022;57(5):533-9. https://doi.org/10.1093/alcalc/agab042

15. Badodekar N, Sharma A, Patil V, Telang G, Sharma R, Patil S, et al. Angiogenesis induction in breast cancer: A paracrine paradigm. Cell Biochemistry and Function. 2021;39(7):860-73. https://doi.org/10.1002/cbf.3663

16. Jain P, Kumar V, Teotia D, Goyal H, Agrawal A, Malik V. Phytochemical Composition of *Sidarhombifolia* ssp. retusa (L.) Bross.: a comprehensive GC/MS analysis. Xi'an Shiyou DaxueXuebao (Ziran Kexue Ban)/Journal of Xi'an Shiyou University, Natural Sciences Edition. 2024;67(1):103-23. https://doi.org/10.5281/zenodo.10578898

17. Jain P, Kumar S, Kumar V, Agrawal A, Teotia D, Kumar A, et al. Unraveling phytochemical diversity and medicinal potential of *Sida rhombifolia* complex: a chemotaxonomic investigation from Northern India. Bioscene. 2024;21(4):572-603.

18. Teotia D, Agrawal A, Kumar V, Jain P, Kumar A, Agrawal B, et al. Ethnobotany, phytochemistry and biological activities of the genus *Allium* L. Environment Conservation Journal. 2025;26(3):1058-76. https://doi.org/10.36953/ECJ.32103049

19. Teotia D, Agrawal A, Goyal H, Jain P, Singh V, Verma Y, et al. Pharmacophylogeny of genus *Allium* L. Journal of King Saud University-Science. 2024;36(8):103330. https://doi.org/10.1016/j.jksus.2024.103330

20. Singla R, Jaitak V. Molecular docking simulation study of phytoestrogens from *Asparagus racemosus* in breast cancer progression. International Journal of Pharmaceutical Sciences and Research. 2015;6(1):172. http://dx.doi.org/10.13040/IJPSR.0975-8232.6(1).172-82

21. Divyalakshmi MV, Thoppil JE. Molecular docking of phytochemicals against breast cancer: a review. Plant Archives. 2022;22(2):163-73. https://doi.org/10.51470/PLANTARCHIVES.2022.v22.no2.029

22. Yang C, Ye Z, Mao L, Zhang L, Zhang J, Ding W, et al. Analysis of volatile organic compounds and metabolites of three cultivars of *Asparagus* (*Asparagus officinalis* L.) using E-nose, GC-IMS and LC-MS/MS. Bioengineered. 2022;13(4):8866-80. https://doi.org/10.1080/21655979.2022.2056318

23. Pedrosa RC, Felipe KB, Wilhelm FD. Oncogenic PI3KT/Akt/mTOR pathway alterations, ROS homeostasis, targeted cancer therapy and drug resistance. Frontiers in Oncology. 2024;14:1372376. https://doi.org/10.3389/fonc.2024.1372376

24. Straley GB, Utech FH. Flora of North America. Vo. 26. FNA. http://www.efloras.org/florataxon.aspx?flora_id=1&taxon_id=102837

25. Linne CV. Car. a Linne Mantissa plantarum: Generum (editionis VI). et specierum editionis II, Impensis Direct. Laurentii Salvii. 1767;1:63. https://doi.org /10.5962/bhl.title.69083

26. Kim S, Chen J, Cheng T, Gindulyte A, He J, He S, et al. PubChem 2025 update. Nucleic Acids Research. 2025;53(D1):D1516-25. https://doi.org/10.1093/nar/gkae1059

27. O'Boyle NM, Banck M, James CA, Morley C, Vandermeersch T, Hutchison GR. Open Babel: An open chemical toolbox. Journal of Cheminformatics. 2011;3:1-14. https://doi.org/10.1186/1758-2946-3-33

28. Berman HM, Westbrook J, Feng Z, Gilliland G, Bhat TN, Weissig H, et al. The protein data bank. Nucleic Acids Research. 2000;28:235-42. https://doi.org/10.1093/nar/28.1.235

29. Morris GM, Huey R, Lindstrom W, Sanner MF, Belew RK, Goodsell DS, et al. AutoDock4 and AutoDockTools4: Automated docking with selective receptor flexibility. Journal of Computational Chemistry. 2009;30(16):2785-91. https://doi.org/10.1002/jcc.21256

30. Daina A, Michielin O, Zoete V. SwissADME: a free web tool to evaluate pharmacokinetics, drug-likeness and medicinal chemistry friendliness of small molecules. Scientific Reports. 2017;7(1):42717. https://doi.org/10.1038/srep42717

31. Huey R, Morris GM, Forli S. Using AutoDock 4 and AutoDock vina with AutoDockTools: a tutorial. The Scripps Research Institute Molecular Graphics Laboratory. 2012;10550(92037):1000.

32. Lindorff-Larsen K, Piana S, Palmo K, Maragakis P, Klepeis JL, Dror RO, et al. Improved side□chain torsion potentials for the Amber ff99SB protein force field. Proteins: Structure, Function and Bioinformatics. 2010;78(8):1950-8. https://doi.org/10.1002/prot.22711

33. Van Der Spoel D, Lindahl E, Hess B, Groenhof G, Mark AE, Berendsen HJ. GROMACS: fast, flexible and free. Journal of Computational Chemistry. 2005;26(16):1701-18. https://doi.org/10.1002/jcc.20291

34. Kagami L, Wilter A, Diaz A, Vranken W. The ACPYPE web server for small-molecule MD topology generation. Bioinformatics. 2023;39(6):350. https://doi.org/10.1093/bioinformatics/btad350

35. Hess B, Bekker H, Berendsen HJ, Fraaije JG. LINCS: a linear constraint solver for molecular simulations. Journal of Computational Chemistry. 1997;18(12):1463-72. https://doi.org/10.1002/(SICI)1096-987X(199709)18:12<1463::AID-JCC4>3.0.CO;2-H

36. Berendsen HJ, Postma JV, VanGunsteren WF, Dinola ARH J, Haak JR. Molecular dynamics with coupling to an external bath. The Journal of Chemical Physics. 1984;81(8):3684-90. https://doi.org/10.1063/1.448118

37. Kumari R, Kumar R, Consortium O, Lynn A. g_mmpbsa-A GROMACS tool for high-throughput MM-PBSA Calculations. Journal of Chemical Information and Modeling. 2014;54(7):1951-62. https://doi.org/10.1021/ci500020m

38. Sloggett C, Goonasekera N, Amp AE. BioBlend: automating pipeline analyses within Galaxy and CloudMan. Bioinformatics. 2013;29(13):1685-6. https://doi.org/10.1093/bioinformatics/btt199

39. Lipinski CA, Lombardo F, Dominy BW, Feeney PJ. Experimental and computational approaches to estimate solubility and permeability in drug discovery and development settings. Advanced Drug Delivery Reviews. 1997;23(1-3):3-25. https://doi.org/10.1016/j.addr.2012.09.019

40. Seeliger D, De Groot BL. Ligand docking and binding site analysis with PyMOL and Autodock/Vina. Journal of Computer-Aided Molecular Design. 2010;24(5):417-22. https://doi.org/10.1007/s10822-010-9352-6

41. Laskowski RA, Swindells MB. LigPlot+: multiple ligand-protein interaction diagrams for drug discovery. Journal of Chemical Information and Modeling. 2011;51(10). https://doi.org/10.1021/ci200227u

42. Agu PC, Afiukwa CA, Orji OU, Ezeh EM, Ofoke IH, Ogbu CO, et al. Molecular docking as a tool for the discovery of molecular targets of nutraceuticals in diseases management. Scientific Reports. 2023;13(1):13398. https://doi.org/10.1038/s41598-023-40160-2

43. Farhad M, Bhuiyan MIH, Uddin SM, Chowdhury MHM, Huda MN, Khan MF, et al. Anticancer potential of isolated phytochemicals from *Ocimum sanctum* against breast cancer: *In silico* molecular docking approach. World Journal of Pharmaceutical Research. 2016;5(12):1232-9. https://doi.org/10.20959/wjpr201612-7511

44. Afrin S, Uddin N, Mehjabin KZ, Niketa TK, Nesa F, Akther S, et al. *In silico* molecular docking approach of some selected isolated phytochemicals from *Phyllanthus emblic* against breast cancer. Biomedical Journal of Scientific & Technical Research. 2018;10(2):1-5. https://doi.org/10.26717/BJSTR.2018.10.001917

45. Majumder M, Khanam T, Rahaman M, Rahimul M, Hossain TN, Chakrabarty N. Anticancer potential of isolated phytochemical from *terminalia bellerica* against breast cancer: *in silico* molecular docking approach. World Journal of Pharmaceutical Research. 2017;6(4):1763-71. https://doi.org/10.20959/wjpr20174-8224

46. Ahmed S, Rakib A, Islam MA, Khanam BH, Faiz FB, Paul A, et al. *In vivo* and *in vitro* pharmacological activities of *Tacca integrifolia* rhizome and investigation of possible lead compounds against

breast cancer through *in silico* approaches. Clinical Phytoscience International Journal of Phytomedicine and Phytotherapy. 2019;5 (1):1-13. https://doi.org/10.1186/s40816-019-0127-x

47. Rizzo LY, Longato GB, Ruiz ALTG, Tinti SV, Possenti A, Vendramini-Costa DB, et al. *In vitro*, *in vivo* and *in silico* analysis of the anticancer and estrogen-like activity of guava leaf extracts. Current Medicinal Chemistry. 2014;21(20):2322-30. https://doi.org/10.2174/09298673216661401201200031
48. Kavitha V, Gunavathy N. Molecular docking studies and orbital analysis to identify anti-cancerous potentials to prevent breast cancer. International Journal of Scientific Research in Computer Science, Engineering and Information Technology. 2017;2(4):2456-3307.
49. Yazdiniapour Z, Sadeghi M, Akbari M, Troiano R, Lanzotti V. Cinnamic acid derivatives from welsh onion (*Allium fistulosum*) and their antibacterial and cytotoxic activities. Phytochemical Analysis. 2021;*32*(1):84-90. https://doi.org/10.1002/pca.2924
50. Teotia D, Malik V. Molecular docking and pharmacokinetic studies of bioactive compounds from methanolic leaf extracts of *Allium hookeri* against alpha amylase & alpha glucosidase. Drug Discovery. 2025;19:e12dd2077. https://doi.org/10.51470/PLANTARCHIVES.2025.v25.no.1.282
51. Majumder R, Parida P, Paul S, Basak P. *In vitro* and *in silico* study of Aloe vera leaf extract against human breast cancer. Natural Product Research. 2018;34(16):2363-6. https://doi.org/10.1080/14786419.2018.1534848
52. Agrawal A, Teotia D, Kumar V, Jain P, Agrawal B, Kumar A, et al. *In silico* identification of antiviral compounds from genus *Asparagus* for chikungunya virus using molecular docking and MD simulation. Plant Archives. 2025;*25*(1):1933-46. https://doi.org/10.51470/PLANTARCHIVES.2025.v25.n
53. Kashyap P, Muthusamy K, Niranjan M, Trikha S, Kumar S. Sarsasapogenin: A steroidal saponin from *Asparagus racemosus* as multi target directed ligand in Alzheimer's disease. Steroids. 2020;153:108529. https://doi.org/10.1016/j.steroids.2019.108529
54. Riaz S, Haider F, ur-Rehman R, Zafar A. Exploring the therapeutic potential of *Asparagus africanus* in polycystic ovarian syndrome: a computational analysis. Journal of Integrative Bioinformatics. 2025;21(4):20240019. https://doi.org/10.1515/jib-2024-0019
55. Li Y, Yang X, Wang F, Zhao J, Zhang C, Wu D, et al. Mechanism of action of *Asparagus officinalis* extract against multiple myeloma using bioinformatics tools, *in silico* and *in vitro* study. Frontiers in Pharmacology. 2023;14:1076815. https://doi.org/10.3389/fphar.2023.1076815
56. Awati SS, Gilhotra RM, Singh SK, Raj V, Wadkar KA. *In vitro* antioxidant potential and cytotoxicity study of *asparagus aethiopicus* l. Extracts on ht-29 human colon cancer cell line. Indian Journal of Pharmaceutical Education and Research. 2020;54:s570-9. https://doi.org/10.5530/ijper.54.3s.156
57. Fareed YYZ, Babu ND, Abdulammer SE. Phytochemical and anthelminthic activity of *Asparagus aethiopicus* L. Journal of Bio Innovation. 2021;10(3):851-62. https://doi.org/10.46344/JBINO.2021.v10i03.15
58. Mokashi AA, Bhatia NM. Exploration of bioactives from natural sources targeting estrogen receptor for breast cancer via *in silico* approach: network pharmacology, molecular docking, MD simulation and DFT studies. Chemistry Africa. 2025;8(2):187-99. https://doi.org/10.1007/s42250-024-01161-4

Additional information

Peer review: Publisher thanks Sectional Editor and the other anonymous reviewers for their contribution to the peer review of this work.

Reprints & permissions information is available at https://horizonepublishing.com/journals/index.php/PST/open_access_policy

Publisher's Note: Horizon e-Publishing Group remains neutral with regard to jurisdictional claims in published maps and institutional affiliations.

Indexing: Plant Science Today, published by Horizon e-Publishing Group, is covered by Scopus, Web of Science, BIOSIS Previews, Clarivate Analytics, NAAS, UGC Care, etc
See https://horizonepublishing.com/journals/index.php/PST/indexing_abstracting

Publisher information: Plant Science Today is published by HORIZON e-Publishing Group with support from Empirion Publishers Private Limited, Thiruvananthapuram, India.